



Original article

Punching shear behavior of LWA bubble deck slab with different types of shear reinforcement

Maha Habeeb*, Adel A. Al-Azzawi, Faiq M.S. Al-Zwainy

Al-Nahrain University, Baghdad, Iraq

ARTICLE INFO

Article history:

Received 4 March 2019

Accepted 5 January 2020

Available online 22 January 2020

Keywords:

Lightweight concrete

Voided slab

Punching shear

Shear reinforcement

LECA

ABSTRACT

Punching shear is the most important problem in flat slabs, which usually requires strengthening for safety reasons. One of the most popular strengthening methods is the employment of shear reinforcement. Also, in order to reduce the self-weight of slabs, lightweight aggregate concrete as well as the bubble deck technology were used in this research. To study the influence of shear reinforcement type on lightweight aggregate voided slab behavior under punching shear, three slabs having the same geometrical and mechanical properties, with different shear reinforcement type (hook, inclined bar and stud) were cast and prepared for testing. As well as a control specimen with no shear reinforcement was used for comparison reason. The results showed that the inclined shear reinforcement has the most positive influence on slab behavior, between the three types of reinforcement that were adopted in the experimental work.

© 2020 The Authors. Production and hosting by Elsevier B.V. on behalf of King Saud University. This is an open access article under the CC BY-NC-ND license (<http://creativecommons.org/licenses/by-nc-nd/4.0/>).

1. Introduction

In a reinforced concrete structure, the span between columns is the main design limitation employed in the building slab systems. To design a larger slab between columns, peripheral beams and/or very thick slabs are required. This will lead to increase the weight of the structure because of requirement for larger amounts of used concrete (Singh and Saini, 2018). The bubble deck technology is the key for solving such construction problems. This technology uses spheres made of recycled industrial plastic to create air voids while providing strength through arch action. It is an attempt for utilizing the positive aspects of concrete slab construction while minimizing the negative attributes of solid slabs by lightening the self-weight of the structure (Chung et al., 2018). Also, lightweight aggregate concrete can be used to produce lighter weight structures.

The most dangerous areas of two-way solid and voided slabs are the slab–column connection area and zones where concen-

trated loads act (Habibi et al., 2014). The concentrated shear force and the large amount of shear stresses in this area cause punching of the concrete slab (Acciai et al., 2016, Sprince et al., 2014; Caratelli et al., 2016). Voided slabs design procedures are more conservative than solid slabs to punching shear failure because of the presence of voids which lead to insufficient cross section area of concrete that was remaining to withstand the shear stresses that generated within this region. Furthermore, lightweight concrete in general shows properties that are weaker than the normal weight concrete. In such cases, shear reinforcement may be enhance the punching shear capacity for the concrete slab (Vainiunas et al., 2015). The punching area of voided slab also can be reinforced with shear reinforcement. In such techniques the shear reinforcement must be provided in the ribs (Valivonis et al., 2017).

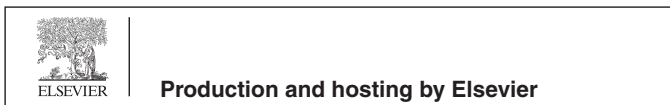
Many experimental investigations were conducted earlier on voided slab. But, there is no available research study on the behavior of lightweight concrete voided slab has been carried out yet.

2. Experimental work

A full scale flat slab system with dimensions of (7.5*7.5) m and supported on columns only, represents the prototype in this research. The zero-moment axes of the selected prototype lies approximately at (0.22 L) from the column axis. The punching shear specimen in this research represent the column strip with scale of 1/3 which exposed to punching shear due to column with square cross section. The column has scaled dimension equals to

* Corresponding author.

E-mail addresses: eng.maha97@yahoo.com (M. Habeeb), dr_adel_azzawi@yahoo.com (A.A. Al-Azzawi), faiqalzwainy@eng.nahrainuniv.edu.iq (F.M.S. Al-Zwainy).
Peer review under responsibility of King Saud University.



(100*100) mm. The experimental work consists of four two way flat slab specimens, simply supported at their edges, with dimension equal to (1100*1100*100) mm and designed to fail in punching shear.

2.1. Materials

2.1.1. Lightweight aggregate

Lightweight aggregate structural LECA (0–8 mm) was used to produce the concrete for all specimens. Its bulk dried density equal to 740 kg/m³. The LECA pebbles internal cellular structure with thousands of air-filled cavities gives thermal and sound insulation properties as shown in Fig. 1. It is chemically neutral, with pH of (7–7.2). It does not affect or be affected by other materials, and even preserves materials intact from chemical hazards (LECA).

2.1.2. Reinforcement

In order to achieve punching failure and prevent bending effect in slab specimens, constant flexural reinforcement (which was more than what normally used in practice) was selected and implemented. Steel bar of 10 mm in diameter, spaced at 65 mm in two directions was used. For punching Shear, three different types of reinforcement were used as detailed below:

1 Hook reinforcement.

Three vertical bars 6 mm in diameter, mechanically anchored at each ends at an angle of 90 degrees were used. Each three bars were welded on via hooks to steel rail have the dimension (200*12.5) mm as shown in Fig. 2. Reinforcement arranged at three-control perimeter lies at 0.5d, d and 2d from column face were prepared as shown in Fig. 3.

2 Stud reinforcement

Depending on ACI318-14 code requirement (ACI 318, 2014), four shear stud with high (6 cm) and stud shank diameter (1.5 cm), welded onto a metal strip measuring (200*12.5) mm at (3 cm) interval was used as shown in Fig. 4.

Steel arm trim at 45°

Inclined steel bars making an angle of 45 degrees with the longitudinal axis of the specimen and crossing the plane of the potential shear crack were used as shear reinforcement. The form consists of three parts, which provides inclined shear reinforcement at critical region where the potential shear crack assumed to extend. The first form lies at region start from column face to (1.5d). While, the second form sets the shear reinforcement at the second critical region which extends from (0.75d) to (2.25d). The third one is provided at the third critical region, which lies between (1.5d-3d). This arrangement provides three shear reinforcement bars crossing the plane of the potential shear crack.

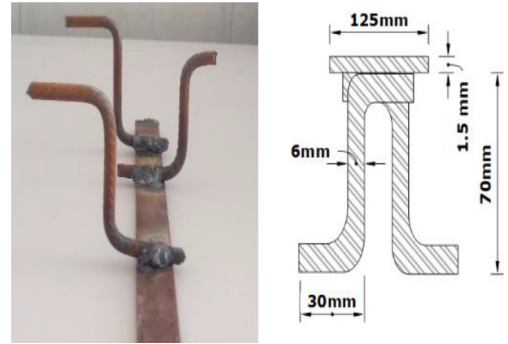


Fig. 2. Shear reinforcement.

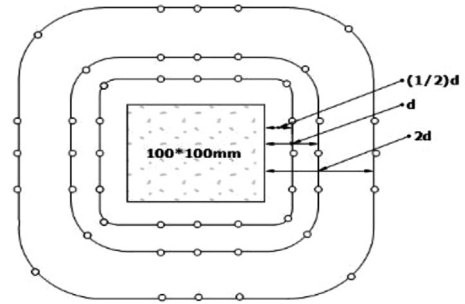


Fig. 3. Shear reinforcement Arrangement.

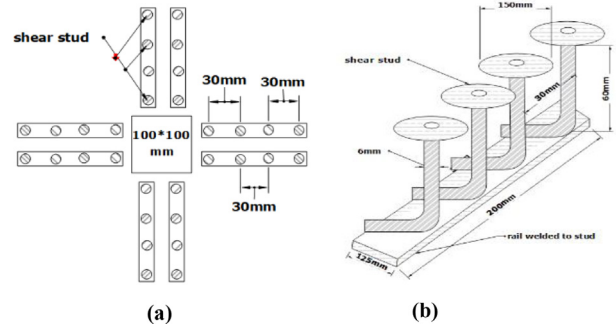


Fig. 4. (a) Shear stud, (b) Shear stud arrangement.



Fig. 5. Shear reinforcement.



Fig. 1. (a) Ordinary leca. (b) Structural leca.

Every single forms were formed as square with line length (100,210,325) mm respectively using steel rail have the dimension (200*12.5) mm. ϕ 6 mm steel bar mechanically anchored at one ends with an angle of 45 degrees was welded on via hook to the steel rail. All details are shown in Figs. 5 and 6.

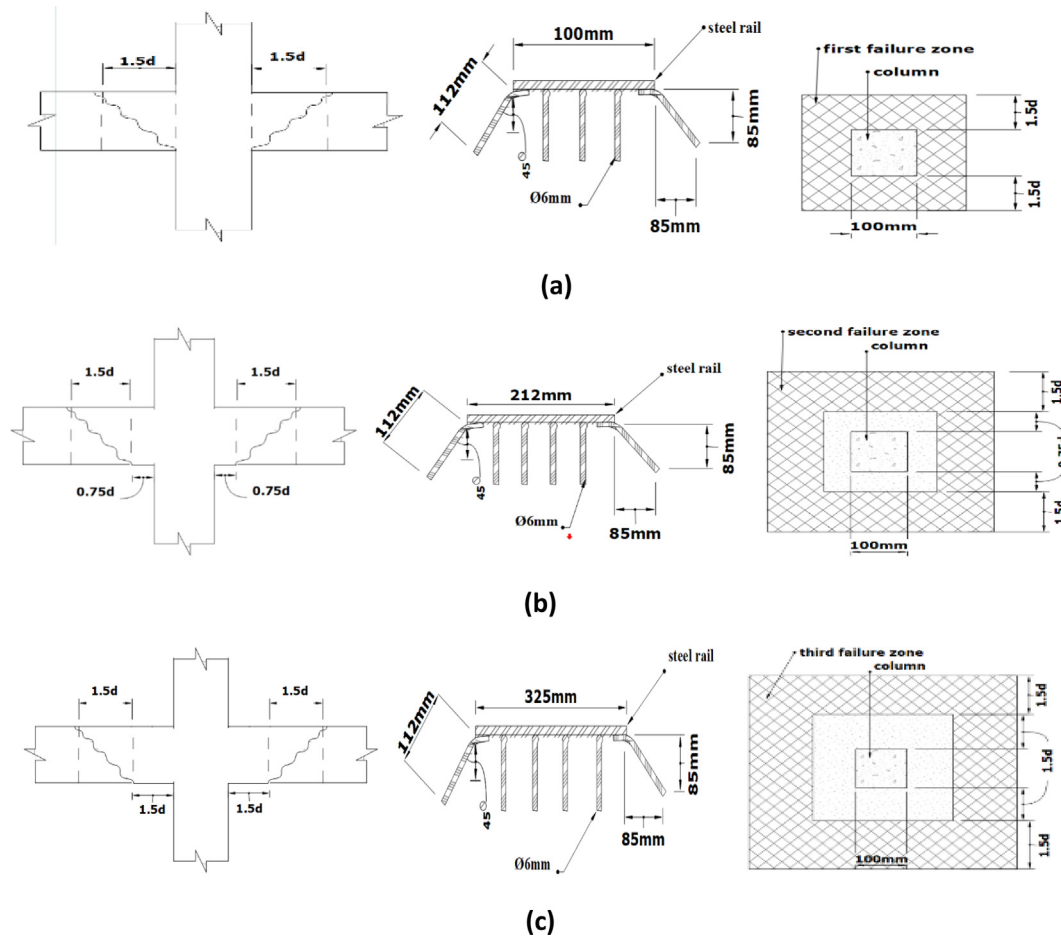


Fig. 6. Shear reinforcement details.

2.1.3. Plastic spheres

Oval spheres with dimensions of (80*80*40) mm made from plastic were manufactured and used. The voids should be covered by concrete from all directions with at least one ninth of the ball diameter before continuing casting (Bubble Deck Head Office, 2008).

2.2. Materials mechanical properties.

Lightweight aggregate concrete, which consists of ordinary Portland cement, natural sand, LECA and high performance

concrete hyper plasticizer Epsilon HP 580 were used for casting all specimens. Table 1 shows concrete mix proportion.

To obtain the mechanical properties of the hardened concrete a laboratory testing of concrete cubes and cylinders must be carried out. A (150 × 150 × 150 mm) cubic samples and standard concrete cylinders with dimension (150 × 300 mm) where tested to obtain the compressive strength (fcu) according to BS1881-116 (Eurocode 2, 2004) and split tensile strength according to ASTM C496 (ASTM C496, 2004). Also, a Prism concrete specimen with dimension (100*100*400) mm where tested to determine the flexural strength capacity according to (ASTM, C78) (ASTM, C78, 2010),

Table 1
Lightweight concrete mix proportion.

Concrete type	Compressive Strength (fc), MPa	Cement Content, Kg/m ³	Sand Content, Kg/m ³	LECA Content, Kg/m ³	Water L/m ³	HP580 L/m ³
lightweight	40	550	550	500	133	0.57

Table 2
Specimens' mechanical properties and details.

No.	Labeling	Slab thickness t (mm)	Shear reinforcement	Bubble diameter D (mm)	Void ratio %	Compressive strength (fcu) MPa	Split tensile strength Fr (MPa)	Flexural strength Ft (MPa)	Modulus of elasticity Ec (MPa)	Reduction in weight due to voided %	Reduction in weight due to lightweight concrete %	Total reduction %
1	BLW 1	100	Without	80*80*40	20.9	39.8	3.1	2.0	11,671	20.95	36.34	57.3
2	BLW 2	100	With hook	80*80*40	20.1	39.6	3	2.01	10,769	20.06	36.37	56.4
3	BLW3	100	With inclined	80*80*40	20.1	43.6	3.7	2.51	11,674	20.06	34.03	54.1
4	BLW4	100	With stud	80*80*40	20.1	37.2	2.8	1.8	10,196	20.06	35.60	55.7

Where: BLW/bubble lightweight concrete specimen.

and the cylindrical samples also was tested to find modulus of elasticity according to ASTM C469/10 (ASTM C469, 2010). Specimen's details and mechanical properties are shown in Table 2.

2.3. Punching shear models

The behaviors of four specimens with simple support having the same geometrical and mechanical properties differ only in shear reinforcement was obtained as shown in Fig. 7. The comparison aims to study the influence of shear reinforcement type on punching shear slab resistance.

2.4. Test setup and measurements

The specimens were tested under a static load by using a universal testing machine with maximum load equal to (1000 kN). The load was applied in load control mode at loading rate of 5 kN/min.

Vertical deflection due to specimen loading was measured at three points located at center of the tested slab (0.5L) on the tension face while the other two point located at distance (0.375L, 0.25L) from the support center on the compression face. Fig. 8 shows loading setup and Fig. 9 shows the specimen after test.

3. Test results

In the ACI318-14 code, the critical section is parallel to the column face at a distance equal to half the effective depth of the slab (ACI 318, 2014). While in the Euro code, the critical section is

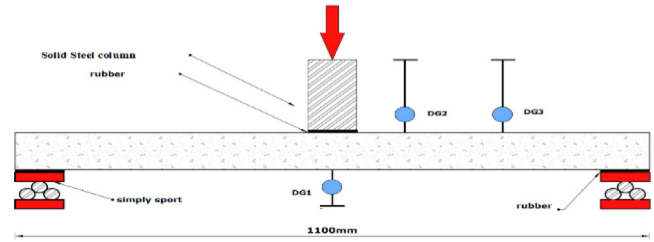


Fig. 8. Punching shear test setup.

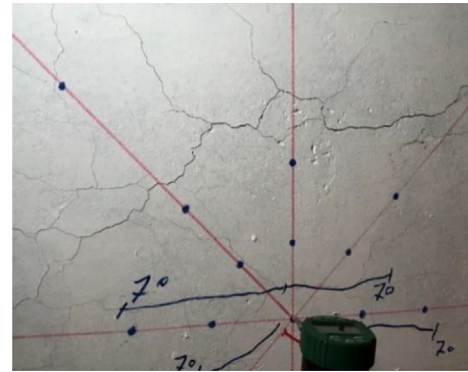


Fig. 9. Punching shear specimen after test.

assumed to be at 1.5d to 2.0d from the face of the column (Eurocode 2, 2004). Critical distances between 0.5d- 2d were studied in this research.

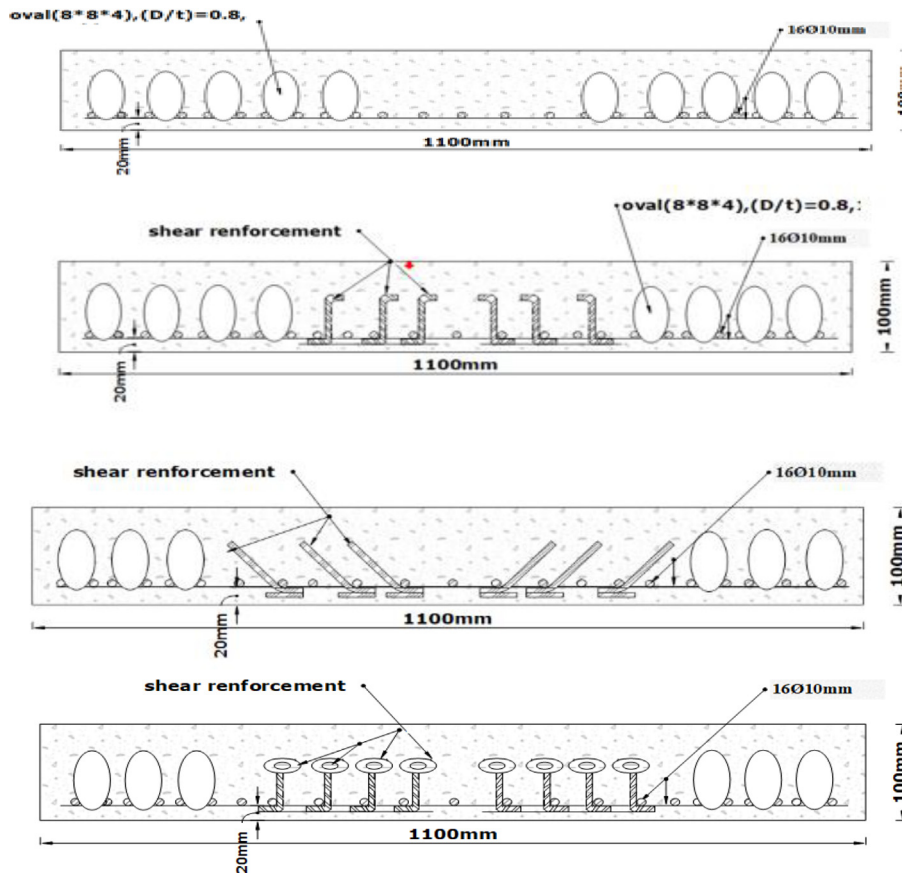


Fig. 7. Specimens' details.

Table 3
Specimens' ultimate load and maximum deflection.

No.	Labeling	Slab Thickness t (mm)	shear reinforcements	bubble diameter	voided %	d/t*	Compression strength	Pu ultimate load	Deflection at ultimate load	Max. deflection
1	BLW 1	100	without	80°80°40	20.9	0.8	39.8	79.1	5.89	12
2	BLW 2	100	With hook	80°80°40	20.1	0.8	39.6	84.8	3.4	8
3	BLW3	100	With inclined	80°80°40	20.1	0.8	43.6	97.8	3.82	7.89
4	BLW4	100	With stud	80°80°40	20.1	0.8	37.2	72.3	2.81	8.59

Where: d, is the void diameter, t, is the slab thickness.

3.1. Ultimate load capacity and maximum Deflection:

Table 3 shows ultimate load and maximum deflection for all specimens.

1. The increase in ultimate load capacity due to shear reinforcement existence with respect to control specimen (BLW1) is found to be (7.2%) for specimen with hook shear reinforcement. This increase was (23.6%) for specimen with inclined shear reinforcement. On contrariwise to that, the capacity for specimen with stud shear reinforcement is found to be lowered by

(8.6%). This may be due to the position of inclined shear reinforcement and the fact that it is located perpendicular to shear crack path.

2. Also, the deflections at ultimate load were compared for all specimens. The results showed that even though the void ratio is the same and equal (20%), the shear reinforcement existence leads to reduce the deflection magnitudes at ultimate load by (42.3%, 35.1% and 52.3%) for (BLW2, BLW3 and BLW4) specimen respectively with regard to the control specimen (BLW1). Then the reduction percent decreased gradually until it reaches the failure deflection to become (33.3%, 34.3% and 28.4%) with respect to the reference slab respectively.

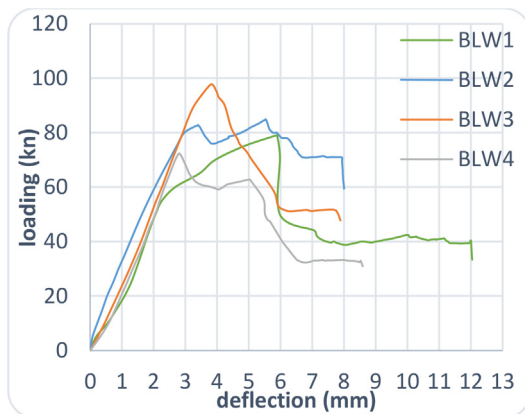


Fig. 10. Load-central deflection curves for case one specimen.

3.2. Load deflection curve:

The central deflection values are plotted against loading for all models together and individual to explain the differences in behavior more clearly as shown in Figs. 10 and 11 respectively.

The load–deflection curves in general at the beginning, showed almost identical behaviors which seem to be straight with linear relationship until reaching the peak load. This may be attributed to the symmetry for all specimens in geometry, supports nature and arrangement and applied load. Although, there is a clear difference between the magnitude of maximum load and deflection that occurred before failure because it depends on slab stiffness. All specimens with shear reinforcement before reaching failure load showed lesser deflection at the same load level compared to the control specimen (BLW1).

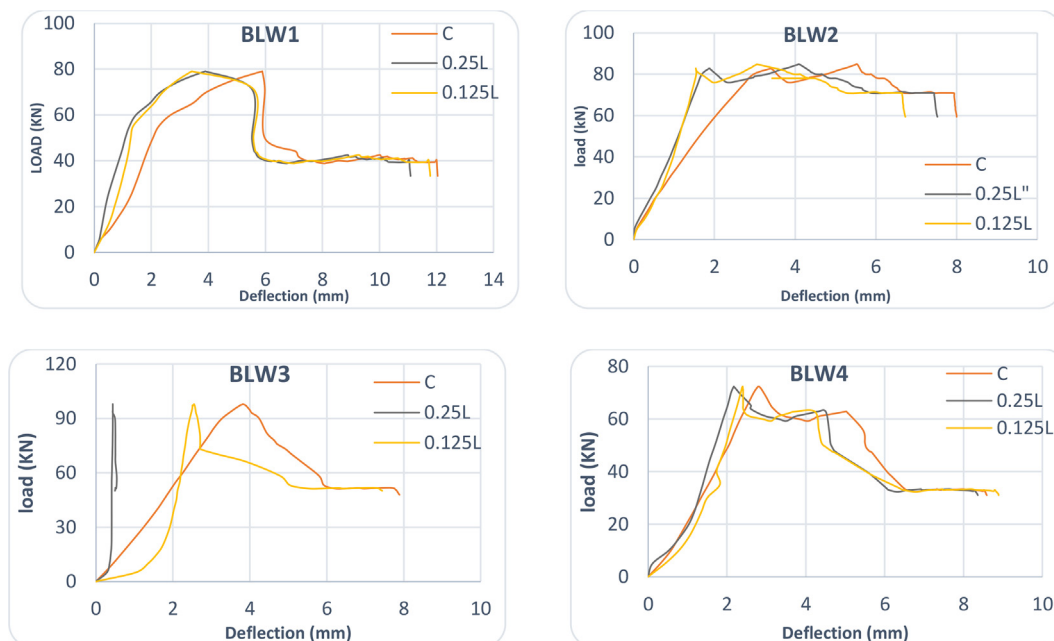


Fig. 11. Load deflection curve for individual specimen.

Table 4
Toughness and deformation factor.

Labeling	Toughness (kN*mm)	Cracking load (KN)	Deflection at first crack (mm)	Ultimate load (kN)	Deflection at ultimate load (mm)	Deformation factor $\frac{\Delta u - \Delta cr}{\Delta u} * 100$
BLW 1	3633.3	57	2.5	79.1	5.9	58.1
BLW 2	1702.2	54.0	1.8	84.8	3.4	48.2
BLW 3	3893.0	79.0	2.9	97.8	3.8	24.1
BLW 4	1730.8	48.0	1.9	72.3	2.8	32.4

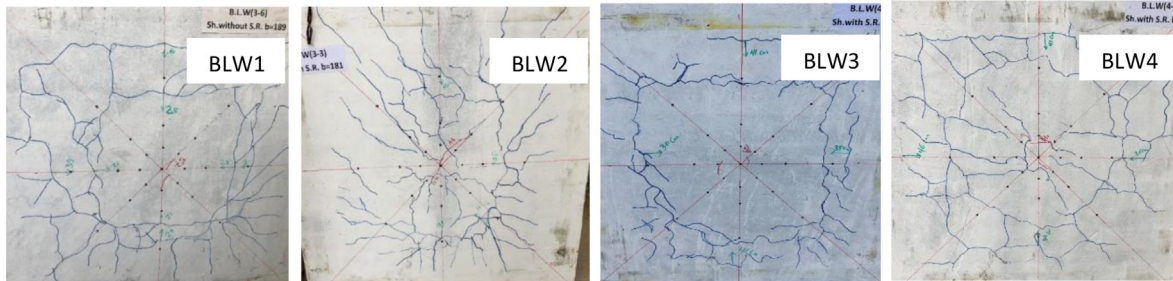


Fig. 12. Crack pattern for all specimens.

The control specimen (BLW1) with no shear reinforcement showed a ductile failure mode accompanied with sudden drop in load-carrying capacity. For the specimen with hook shear reinforcement (BLW2), the load deflection curve showed clear difference in behavior as it is approaching the failure load. The model showed erratic behavior, there is no sudden failure, and no rapid change in deflection magnitude. In terms of strength, the slab with inclined shear reinforcement (BLW3) showed a slightly better performance. After reaching the ultimate load the load deflection curve showed a quick drop in load carrying capacity with gradually increase in deflection. Finally, the bubble lightweight specimen with stud shear reinforcement (BLW4), showed a behavior closer to (BLW2) where the loss of load carrying capacity occurred gradually.

3.3. Toughness and plastic deformation

The material toughness is the maximum amount of energy it can absorb before fracturing (ASTM C1018, 2006). The term

“toughness” represented by the area of the post-cracking region under the load deflection curve. The percent of deflection that accord after first crack was calculated to measure specimen’s ability to show significant deformation before rupture. Table 4 shows the toughness value and deformation factor for all specimens.

$$\text{Deformation factor} = \frac{\Delta u - \Delta cr}{\Delta u} * 100$$

The results show that:

1. For the same void ratio the existence of steel reinforcement decreases the amount of absorbed energy by (53.2%) for slab with hook reinforcement (BLW2) and (52.4%) for slab with stud reinforcement (BLW4). For specimen with inclined shear reinforcement (BLW3), the absorb energy increases to reach (107.2%) with respect to energy of slab without shear reinforcement. So, (BLW3) with inclined shear reinforcement showed an increase in absorbed energy equals to (55%) with respect to other shear reinforcement type.

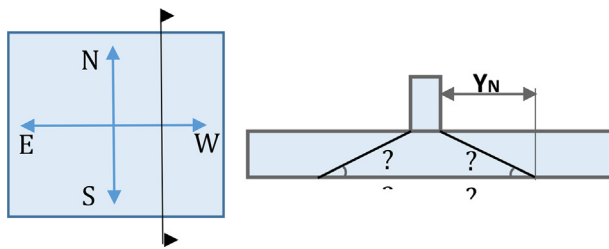


Fig. 13. Punching shear failure angle.

3.4. Crack pattern

The punching shear force transferred from column through surrounding concrete slab. Immediately after the stresses with in concrete reach the ultimate tensile stress, first crack is formed. When the loading continue to increase, the other cracks start to form at the slab central region. After that, the cracks extends away from the area where high value of tensile stresses towards the edges of the slab where low stresses existence until rupture accord. Because of void existence, the failure parameter was in the first row of voids

Table 5
Critical perimeter and failure angles.

Labeling	Y _N (mm)	Y _S (mm)	Y _E (mm)	Y _W (mm)	Perimeter (mm)	Failure Angles			
						??N	??S	??E	??W
BLW 1	210	160	170	200	1880	25.5	32	30.5	26.6
BLW 2	200	230	-	180	1420	26.6	23.5	-	29
BLW 3	230	270	250	220	2340	23.5	20.3	21.8	24.4
BLW 4	290	230	260	290	1995	19	23.5	21	19

Where: Y the distance from column face to failure crack in different direction as shown in Fig. 13.

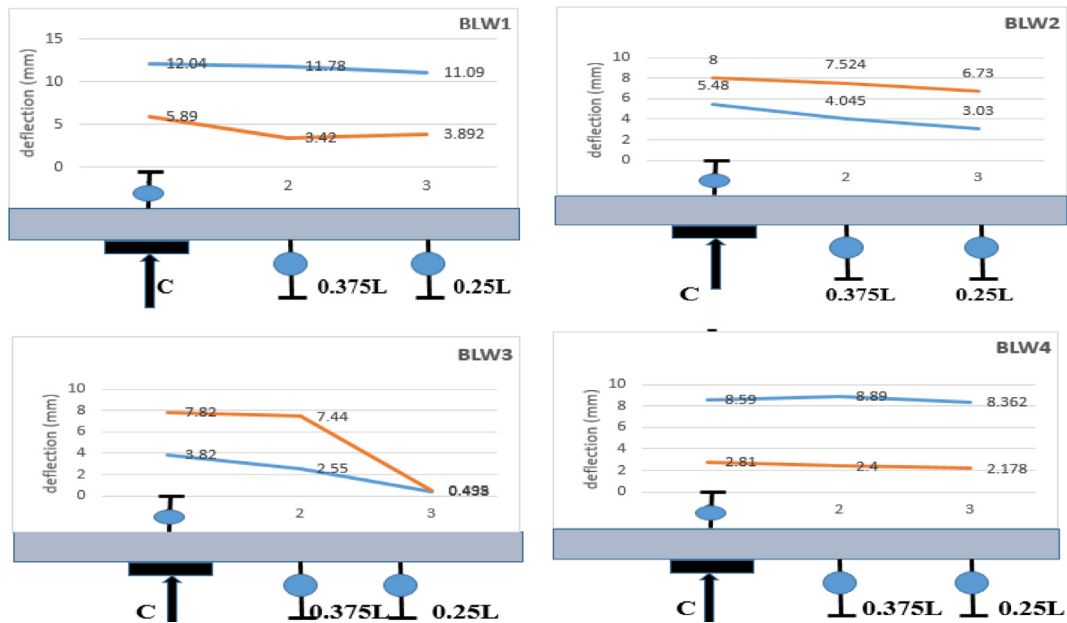


Fig. 14. Failure zone.

at distance $2d$ from column face. Flexural cracks are noticed on the compression side. Then failure accord in tension face without damaged zone. That is leads to approximately same crack pattern with circular or rectangular parameter. Fig. 12 shows cracks pattern for all specimens.

3.5. Failure zone and failure angles

The mode of punching failure was typically pyramid in shape. Which produce an angle (θ) with the tension face of the slab. The specimens have plan direction named (N, S, E, W) which represent (north, south, east, west) directions see Fig. 13. Table 5 shows the failure angle value for all specimens. The control specimen (BLW1) with no shear reinforcement has the largest angle with two failure cracks. While, the (BLW4) slab showed the smallest failure angle with a single shear crack. The (BLW3) slab has the largest critical parameter value.

From Fig. 14, the solid area around the column was deflected at the same rate for all specimens except (BLW3). Shear stresses was concentrated at the first row where the voids exist until the failure occurrence at that critical region. For (BLW3) slab the shear crack generated under the skin of compression face of the slab. The crack continues to develop around the shear reinforcement. Depending on the shear reinforcement geometry, the failure occurred at distance $d/2$ beyond the outer layer of shear reinforcement.

4. Conclusion

1. In general, for lightweight aggregate concrete slab shear reinforcement existence leads to reduce the deflection at ultimate load by at least 35% with respect to slab without shear reinforcement
2. All specimens with shear reinforcement before reaching failure load showed lesser deflection at the same load level compared to the control specimen without shear reinforcement.
3. For the same void ratio, the existence of hook or stud shear reinforcement decreases the amount of absorbed energy by at least 50%. While for slab with inclined shear reinforcement, the absorb energy is increased to reach (107.2%) with respect to energy of slab without shear reinforcement.

4. The inclined shear reinforcement has the most positive effect on lightweight voided slab behavior in terms of ultimate load, deflection, and slab toughness because the inclined reinforcement located perpendicular to the potential shear crack path. This causes a clear reduction in the effect of shear stresses on the column-slab connection region.
5. The punching shear capacity for lightweight aggregate concrete may be significantly improved by using devolved reinforced concrete shear reinforcement rather than using traditional one.

Declaration of Competing Interest

The authors declare that they have no known competing financial interests or personal relationships that could have appeared to influence the work reported in this paper.

References

- Acciai, A., D'Ambrisi, A., Stefano, M. De, Feo, L., Focacci, F., Nudo, R., 2016. Experimental response of FRP reinforced members without transverse reinforcement: failure modes and design issues. *J. Compo. Part B Eng.* 89, 397–407.
- ACI 318, 2014. Building code requirements for structural concrete. American Concrete Institute, Farmington Hills, USA.
- ASTM C496, 2004. Standard test method for splitting tensile of cylindrical concrete specimens. Annual book of ASTM Standards, 4, 259–262.
- ASTM C1018, 2006. Standard test method for flexural toughness and first-crack strength of fiber-Reinforced concrete. Annual book of ASTM Standards
- ASTM, C78, 2010. Standard test method for flexural strength of concrete (using simple beam with third-point loading). Annual book of ASTM Standards.
- ASTM C469, 2010. Standard test method for static modulus of elasticity and Poisson's ratio of concrete in compression. Annual book of ASTM Standards.
- Bubble Deck Head Office UK, 2008. Bubble deck voided flat slab solutions. Technical Manual and Documents. UK.
- Caratelli, A., Imperatore, S., Meda, A., Rinaldi, Z., 2016. Punching shear behavior of lightweight fiber reinforced concrete slabs. *Compos. Part B Eng.* 99, 257–265.
- Chung, J.H., Jung, H.S., Bae, B., 2018. Two way flexural behavior of donut-type voided slabs. *Int. J. Conc. Struct. Mater.*, 12(26)
- Eurocode 2 - BS EN 1992-1-1:2004, published by the British Standards Institution (BSI).
- Habibi, F., Cook, W.D., Mitchell, D., 2014. Predicting post-punching shear response of slab-column connections. *ACI Struct. J.* 111 (1), 123–134.
- LECA, <https://www.leca.co.uk/properties-of-leca>.
- Vainiunas, P., Šalna, R., Šakinis, D., 2015. Probability based design of punching shear resistance of column to slab connections. *J. Civ. Eng. Manag.* 21, 804–812.

Valivonis, J., Skuturna, T., Daugevičius, M., Šneideris, A., 2017. Punching shear strength of reinforced concrete slabs with plastic void formers. *Constr. Build. Mater.* 145, 518–527.

Singh, M., Saini, B., 2018. Analytical and Experimental Study of Voided Slab. Proceedings of the first International Conference on Sustainable Waste

Management through Design. ICSWMD. Lecture Notes in Civil Engineering, 21. Springer, Cham.

Sprince, A., Fischer, G., Pakrastinsh, L., Korjamins, A., 2014. Crack propagation in concrete with silica particles. *Adv. Mater. Res.* 842, 470–476.